High-Pressure Raman Study of Debundled Single-Walled Carbon Nanotubes

U. Schlecht,[a] U. D. Venkateswaran,[b,*] E. Richter,[c] J. Chen,[d] R. C. Haddon,[e] P. C. Eklund,[f] and A. M. Rao[g,*]

[a] Max Planck Institute for Solid State Research, 70569 Stuttgart, Germany
[b] Department of Physics, Oakland University, Rochester, Michigan, USA
[c] Department of Physics & Astronomy, University of Kentucky, Lexington, Kentucky, USA
[d] Zyvex Corporation, Richardson, Texas, USA
[e] Department of Chemistry, University of California, Riverside, California, USA
[f] Department of Physics, Pennsylvania State University, University Park, Pennsylvania, USA
[g] Department of Physics and Astronomy, Clemson University, Clemson, South Carolina, USA

We report the pressure dependence for the radial (ω_R) and tangential (ω_T) band frequencies in debundled single-walled carbon nanotubes (SWNTs) derived from laser-synthesized SWNT bundles. As previously described, a chemical procedure was used to prepare debundled SWNTs from as-prepared, large SWNT bundles. The normalized pressure coefficient for ω_R in the debundled sample was compared with the corresponding value in the bundled sample to quantify the strength of van der Waals interactions between tubes in these nanotube materials. Furthermore, the pressure dependences for the radial (ω_R) and tangential (ω_T) band frequencies in debundled tubes were also compared with corresponding dependences predicted for isolated SWNTs, obtained with generalized tight binding molecular dynamic (GTBMD) simulations described in our previous work. The results presented here collectively suggest that the van der Waals interaction is still strong in the debundled sample studied here, which contained predominantly small bundles of SWNTs rather than isolated tubes.

Keywords: Single-Walled Carbon Nanotubes, Raman Spectroscopy, Debundled SWNTs.

1. INTRODUCTION

The study of Raman-active modes in single-walled carbon nanotubes (SWNTs) as a function of external pressure has been used extensively to probe the influence of van der Waals (vdW) interactions on the vibrational modes in carbon nanotubes[1−5] and the pressure-induced structural transitions in SWNTs.[3,5] Pressure-induced changes in the electrical[6] and optical[7] properties of SWNT bundles have also been reported. In the high-pressure experiments reported to date,[1−7] SWNT material synthesized either by the electric arc (EA)[8] or pulsed laser vaporization (PLV)[9] methods has been used. From transmission electron microscopy and X-ray diffraction measurements, these SWNT materials are found to contain bundles in which ∼100 SWNTs are held together in a triangular lattice by vdW forces, with the most dominant tube diameter around 1.3–1.4 nm.

The Raman spectrum of SWNT bundles collected at ambient pressure exhibits two prominent bands, a low-frequency band in the region of 160–180 cm^{-1} (radial band) and a high-frequency band at ∼1590 cm^{-1} (tangential band). While the frequency of the tangential band, ω_T, is nearly independent of the tube diameter, the radial band frequency, ω_R, depends inversely on the tube diameter.[10,11] The frequency position (and/or lineshape) of these bands has been reported to be sensitive to excitation wavelength,[10−12] external pressure,[1−5] dopant type,[13] and the size of the bundle.[14] Our previous work using generalized tight binding molecular dynamic (GTBMD) simulations predicted different pressure dependences for ω_R in bundled and isolated tubes.[1] These GTBMD calculations showed that the pressure dependence for ω_R is sensitive to the coupling between the tubes in the SWNT bundles. To determine experimentally the pressure dependence for ω_R and ω_T in nearly isolated tubes and to compare the results with the GTBMD calculations, debundled SWNT samples were prepared by a chemical method that was reported previously.[15]

2. EXPERIMENTAL DETAILS

Large SWNT bundles (containing more than 100 tubes) produced by pulsed laser vaporization of graphite were debundled by chemical methods described in Ref. 15. This procedure resulted in some isolated tubes, but the majority of the tubes were in small bundles containing three to seven tubes, as seen in the height profile analysis
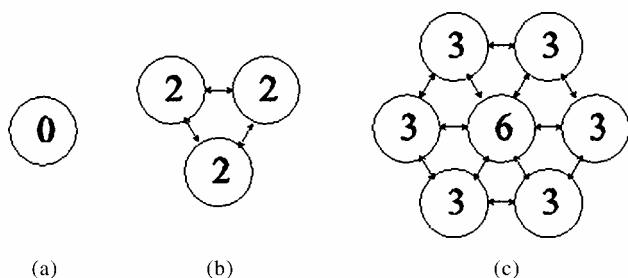
Fig. 1. Schematic representation of small bundles present in the debundled SWNT samples used in this study. Each circle represents a nanotube, and the numbers inside the circles indicate the number of neighboring nanotubes.

Fig. 2. Three scenarios by which the external pressure can be transmitted to bundled SWNTs (see text). The arrows indicate the direction of applied pressure. (I) External pressure on SWNT bundle only. (II) Isotropic pressure on each tube and vdW interaction between tubes is absent. (III) Same as (II), but vdW interaction between tubes is present.

of AFM images. (AFM and TEM images of debundled tubes can be found in Refs. 15 (*J. Phys. Chem. B*) and 16, respectively.) A schematic representation of the debundled SWNT sample containing a smaller number of tubes is shown in Figure 1, where the number within the tube represents the number of neighboring tubes. For example, an isolated tube has zero neighboring tubes (Fig. 1a), within a bundle of three tubes each tube has two neighboring tubes (Fig. 1b), and the peripheral tubes in a bundle of seven tubes have three neighboring tubes, whereas the central tube has six neighboring tubes (Fig. 1c). The samples were soluble in organic solvents such as CS_2 and THF. The samples for the study reported here were prepared in the solid form by evaporation of the solvents. A tiny flake ($\sim 0.10 \times 0.10$ mm^2) of the debundled SWNTs was loaded into a gasketed diamond anvil cell together with a ruby chip for pressure calibration and a 4:1 mixture of methanol:ethanol as the pressure-transmitting medium. Room-temperature Raman data were obtained at elevated pressures in the range of 0–4.8 GPa with 514.5-nm excitation from an argon ion laser, with an HR 460 spectrometer equipped with a liquid nitrogen-cooled CCD (Instruments SA, Inc.). The cell pressure was determined with standard ruby luminescence.[17]

3. RESULTS AND DISCUSSION

In the GTBMD scheme, a Lennard-Jones-type potential was used to describe the vdW forces between SWNTs in a bundle, with parameters similar to those needed to simulate the *c*-axis bonding in bulk graphite. In the calculations, the hydrostatic pressure, P, was introduced through a radial force, $F_P = P \cdot A$, where A is a cross-sectional area, perpendicular to the tube axis.[1] To interpret the experimental data of Ref. 1, three scenarios (I, II, and III) by which the external applied pressure can be transmitted to the SWNT bundles were considered. They are shown schematically in Figure 2. In model I, the pressure-transmitting liquid resides external to the SWNT bundle and pressure is transmitted only to the outer tubes, and the tubes in the interior of the bundle are coupled to the external force through vdW interactions. Model II describes a
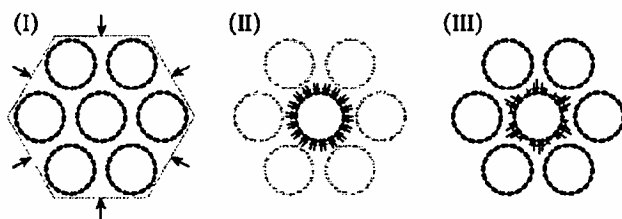
situation in which the vdW interactions are neglected and the pressure-transmitting liquid penetrates the bundle via the interstitial channels to exert uniform pressure on individual tubes within the bundle. This model also applies to isolated tubes, where the pressure-transmitting liquid can freely access the entire perimeter of each tube and the vdW interactions are thereby strongly reduced. Finally, model III is identical to model II, except for the inclusion of the vdW interactions in the GTBMD calculations.

The Raman spectra in the region of the radial and tangential bands in debundled SWNTs measured at various pressures are shown in Figure 3a and b, respectively. With increasing pressure, both the radial and tangential band frequencies shift to higher values with a concomitant decrease in their band intensities and an increase in their linewidth. The radial band could not be detected above ~ 3 GPa, whereas the tangential band was detected up to the highest cell pressure (4.8 GPa) used in this study. The smooth curves superimposed over the experimental data in Figure 3a and b represent fitted Lorentzian lineshapes. A single, broad Lorentzian sufficiently describes the lineshape for the radial band, whereas at least two Lorentzians (labeled T_1 and T_2) were needed for the tangential band. For tubes in the diameter range of $1.0 < d < 1.6$ nm, and using a 514.5-nm excitation wavelength, we expect to excite primarily semiconducting tubes.[12] Analyses of the pressure-induced changes in the linewidths for the radial and tangential bands showed that in the case of bundled and debundled samples, the linewidths remain more or less the same up to about 2 GPa and exhibit a supralinear increase for $P > 2$ GPa. The radial band in the bundled tube was observed only for $P < 1.9$ GPa; its linewidth of ~ 15 cm^{-1} compares well with the corresponding values in the debundled SWNT sample. In the case of the tangential band, there is an overall increase of approximately 5 cm^{-1} in the bundled tubes compared with the corresponding linewidths in debundled tubes. Tentatively, we attribute this increase to faceting of tubes within large bundles under pressure.

In Figure 4a and b, we compare, respectively, the pressure-induced frequency shifts of the radial and tangential band frequencies for debundled SWNTs (squares) obtained in this work with those reported previously in
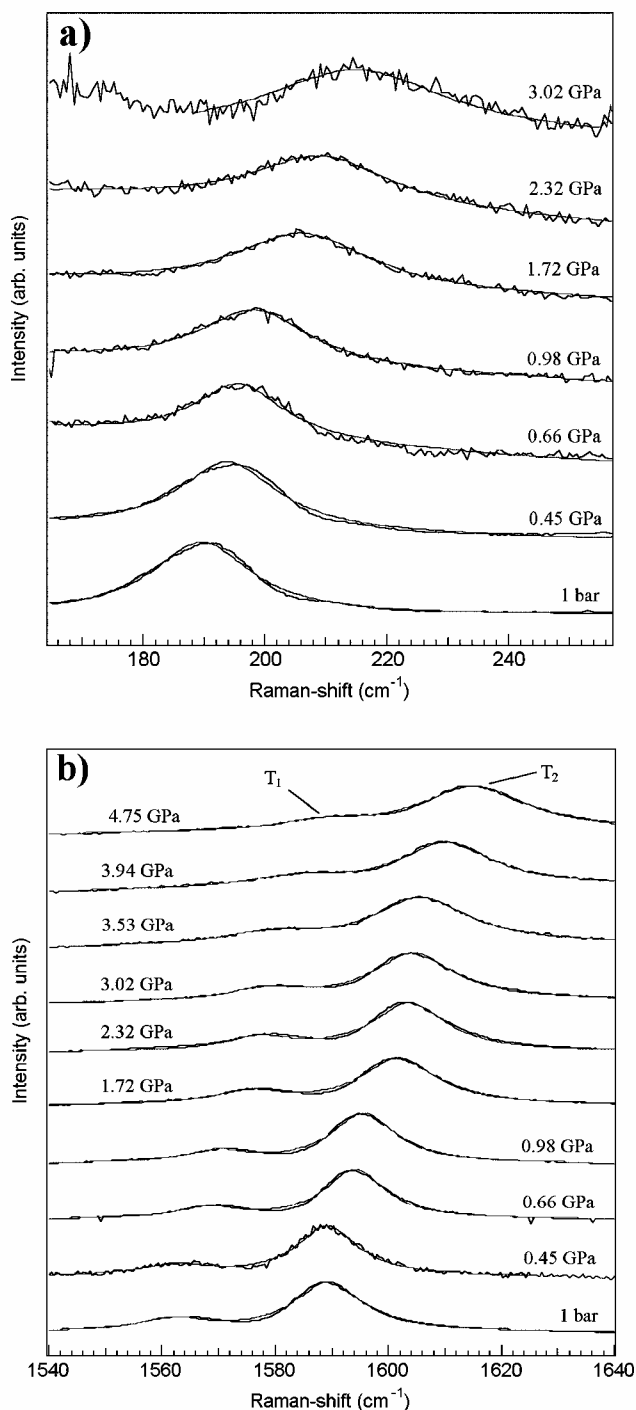
Fig. 3. Raman spectra of the radial (a) and tangential (b) bands observed for debundled SWNTs at the indicated pressure.

Fig. 4. Pressure dependence for ω_R (a) and ω_T (b). Solid symbols represent experimental data for debundled SWNTs (■) from this work and bundled tubes (▲) from Ref. 1. Solid lines correspond to a linear fit in (a) and quadratic fits in (b) for the data. The dashed lines are theoretical pressure dependence predicted by models I–III (see text and Ref. 1).

modes observed in the debundled SWNTs as T_1 and T_2 in Figures 3 and 4; these peaks are the same as those labeled T_2 and T_3 in the case of bundled SWNTs (Figures 1 and 3 of Ref. 1). The solid lines represent fits to the experimental data (linear in Fig. 4a; quadratic in Fig. 4b), whereas the dashed curves represent theoretical pressure dependences for ω_R and ω_T from models I–III of Ref. 1. We find that the experimentally observed pressure dependence for both ω_R and ω_T in debundled SWNTs is nearly the same as in bundled SWNTs.

It should be noted that the GTBMD calculations (see dashed lines in Fig. 4a) predict different pressure dependences for ω_R in bundled (models I and III) and isolated (model II) tubes. For the pressure dependence of ω_R in debundled SWNTs, we obtain an experimentally determined linear shift of $\sim$8.4 cm^{-1}/GPa, which is comparable to the values of 9.7 cm^{-1}/GPa (Ref. 4) and 10.1 cm^{-1}/GPa (Ref. 5) reported, respectively, for $d\omega_R/dP$ in EA-derived and PLV-derived bundled tubes. Thus, the experimentally determined pressure coefficient for ω_R in debundled SWNTs is significantly higher than the pressure dependence of $\sim$1.3 cm^{-1}/GPa for ω_R predicted by model II for isolated tubes. This would suggest that the debundled sample contains predominantly small bundles rather than isolated tubes.

Pressure dependences for ω_R and ω_T have been reported for bundled EA-derived or PLV-derived SWNTs by different research groups. Because of the inherent variation in the tube diameter distribution in the EA- or PLV-derived SWNTs, and consequent variations in ω_R, *normalized derivatives* of ω_R with respect to pressure ($\frac{1}{\omega}\frac{d\omega}{dP}$) are listed in Table I to facilitate a meaningful comparison for the pressure dependence of ω_R in the EA- or PLV-derived SWNTs.

Thomsen et al.[4] used an elasticity model in which a single nanotube is assumed to be a hollow cylinder with a finite wall thickness and isotropic elastic properties.

Ref. 1 for bundled SWNTs (triangles). In this figure, we have plotted the difference between the observed frequency at any given pressure and the atmospheric pressure frequency, $[\omega(P) - \omega(0)]$, along the vertical axis for convenience of comparison. This choice for the ordinate enables us to eliminate the shifts in ω_R between the bundled and debundled SWNTs, which was discussed in Ref. 14. In this paper, we have labeled the two tangential
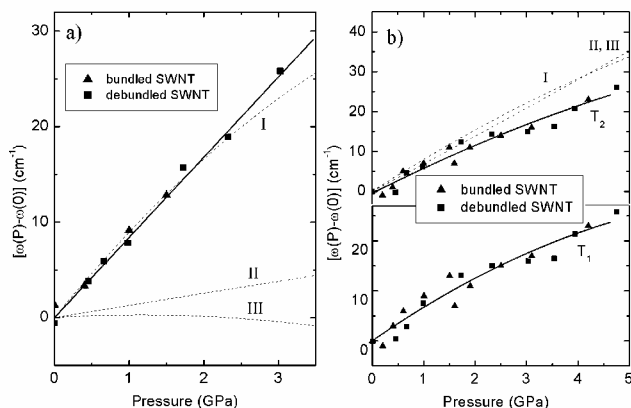
Table I. Comparison of the normalized derivative of ω_R with respect to pressure in SWNT samples obtained in this work and by other research groups.

ω_R at ambient pressure (cm^{-1})	$(d \ln \omega_R / dP)$ (TPa^{-1})	α (%)	Material	Reference
190	44	28	Debundled SWNTs (PLV-derived)	This work
185	48	31	PLV	[1]
172	56	}	EA	[3]
171	57	} 37	EA	[4]
182	56	}	PLV	[5]

α is a measure of the vdW contribution to the normalized derivative of ω_R as stated in Eq. (1) (see text).

From a comparison of strain components in the axial and tangential directions, they calculated that $\frac{1}{\omega}\frac{d\omega}{dP}$ should be twice as high for ω_R as for ω_T. However, the measured ratio of the radial to the tangential normalized pressure coefficients was found to be ~ 16 (Ref. 4). This observed higher ratio led them to suggest two contributions to the pressure coefficient for the radial mode in bundled tubes: one from radial breathing eigenmode of individual tubes, and a second from condition vdW interaction between tubes. Assuming that the force constant for ω_R is the sum of the force constants for a pure radial breathing mode and a pure van der Waals contribution, they separated the logarithmic pressure derivative as

$$\frac{d \ln \omega_R}{dP} = (1-\alpha)\frac{d \ln \omega_{RBM}}{dP} + \alpha \frac{d \ln \omega_{vdW}}{dP} \qquad (1)$$

where α is an estimate of the vdW contribution. Since a SWNT can be viewed as a single graphene sheet rolled into a seamless tube, Thomsen et al. argued that the normalized pressure coefficient of the in-plane (high-frequency E_{2g} mode) and interplane (B_{1g} mode) vibrations in graphite, respectively, can be identified with $d \ln \omega_{RBM}/dP$ and $d \ln \omega_{vdW}/dP$ terms in Eq. (1). Using the values from the high-pressure Raman work by Hanfland et al. on graphite[18], that is, 3.0 (TPa)$^{-1}$ for $d \ln \omega_{RBM}/dP$ and 150 (TPa)$^{-1}$ for $d \ln \omega_{vdW}/dP$, Thomsen et al. obtained $\alpha \sim 37\%$ for bundled SWNTs, suggesting that $\sim 37\%$ of the normalized pressure coefficient for the radial mode arises from intertube interactions.[4] An analysis of experimental data from other groups[3−5] within the framework of Thomsen's model also yields $\alpha \sim 37\%$ for bundled SWNTs (cf. Table I). A similar analysis of the Raman data depicted in Figures 3a and 4a yields $\alpha \sim 28\%$ for debundled SWNTs. The value of α in the debundled SWNTs is only slightly smaller than the value (31%) obtained for the bundled tubes in our previous work. The comparison between the α values found for the debundled tubes in this work and the EA- and PLV-derived SWNT bundles studied by other groups is slightly better (28% vs. 37%; see Table I). Nonetheless,

the reduction in the value of α in the debundled tubes is small, considering that the debundled sample studied here contained only three to seven tubes, whereas the SWNT bundles studied earlier had about 100–200 neighboring tubes. This is a surprising result and warrants further high-pressure Raman studies on a homogeneous sample of isolated SWNTs prepared by either improved chemical methods or chemical vapor deposition. The present study suggests that the magnitude of the vdW interactions on ω_R, as reflected in the pressure dependence of the Raman-active radial breathing mode, is nearly the same whether a SWNT resides within a large bundle (with 100 neighboring tubes) or inside a small bundle containing three to seven tubes.

4. CONCLUSIONS

We have determined the pressure dependence for ω_R and ω_T in debundled SWNTs in the pressure range from 0 to 4.8 GPa and compared them with corresponding dependences in bundled SWNTs and model calculations based on GTBMD simulations. Analysis of our data within the framework of the elasticity model used by Thomsen et al.[4] yielded a relatively high value of $\alpha \sim 28\%$ in debundled SWNTs. Furthermore, in contradiction to the GTBMD predictions, identical pressure dependences for ω_R and ω_T in debundled and bundled SWNTs were obtained. The results of this study collectively suggest that the magnitude of the vdW interactions on ω_R, as reflected in the pressure dependence of the Raman-active radial breathing mode, is nearly the same whether a SWNT resides within a large bundle (with 100 neighboring tubes) or inside a small bundle containing three to seven tubes. Further high-pressure experiments on a homogeneous sample of isolated SWNTs or on a single tube will be important in evaluating the contribution from intertube vdW interaction in SWNT bundles.

References and Notes

1. U. D. Venkateswaran, A. M. Rao, E. Richter, M. Menon, A. Rinzler, R. E. Smalley, and P. C. Eklund, *Phys. Rev. B* 59, 10928 **(1999)**.
2. U. D. Venkateswaran, E. A. Brandsen, U. Schlecht, A. M. Rao, E. Richter, I. Loa, K. Syassen, and P. C. Eklund, *Phys. Status Solidi B* 223, 225 **(2001)**.
3. A. K. Sood, P. V. Teresdesai, D. V. S. Muthu, R. Sen, A. Govindaraj, and C. N. R. Rao, *Phys. Status Solidi B* 215, 393 **(1999)**.

RESEARCH ARTICLE

4. C. Thomsen, S. Reich, A. R. Goñi, H. Jantoljak, P. M. Rafailov, I. Loa, K. Syassen, C. Journet, and P. Bernier, *Phys. Status Solidi B* 215, 435 (**1999**); S. Reich, H. Jantoljak, and C. Thomsen, *Phys. Rev. B* 61, R13389 (**2000**).

5. M. J. Peters, L. E. McNeil, J. P. Lu, and D. Kahn, *Phys. Rev. B* 61, 5939 (**2000**).

6. R. Gaál, J.-P. Salvetat, and L. Forró, *Phys. Rev. B* 61, 7320 (**2000**).

7. S. Kazaoui, N. Munani, H. Yamawaki, K. Aoki, H. Kataura, and Y. Achiba, *Phys. Rev. B* 62, 1643 (**2000**).

8. C. Journet, W. K. Maser, P. Berneer, A. Loiseau, M. Lamy de la Chapelle, S. Lefrant, P. Deniard, R. Lee, and J. E. Fischer, *Nature* 388, 756 (**1997**).

9. A. Thess, R. Lee, P. Nikolaev, H. Dai, P. Petit, J. Robert, C. Xu, Y. H. Lee, S. G. Kim, A. G. Rinyler, D. T. Colbert, G. E. Scuseria, D. Tománek, J. E. Fischer, and R. E. Smalley, *Science* 273, 483 (**1996**).

10. A. M. Rao, E. Richter, S. Bandow, B. Chase, P. C. Eklund, K. A. Williams, S. Fang, K. R. Subbaswamy, M. Menon, A. Thess, R. E. Smalley, G. Dresselhaus, and M. S. Dresselhaus, *Science* 275, 187 (**1997**).

11. S. Bando, W. Asaka, Y. Saito, A. M. Rao, L. Grigorian, E. Richter, and P. C. Eklund, *Phys. Rev. Lett.* 80, 3779 (**1998**).

12. M. A. Pimenta, A. Marucci, S. A. Expedocles, M. G. Bawendi, E. B. Hanlon, A. M. Rao, P. C. Eklund, R. E. Smalley, G. Dresselhaus, and M. S. Dresselhaus, *Phys. Rev. B* 58, R16016 (**1998**).

13. A. M. Rao, P. C. Eklund, S. Bandow, A. Thess, and R. E. Smalley, *Nature* 388, 257 (**1997**).

14. A. M. Rao, J. Chen, E. Richter, U. Schlecht, P. C. Eklund, R. C. Haddon, U. D. Venkateswaran, Y.-K. Kwon, and D. Tománek, *Phys. Rev. Lett.* 86, 3895 (**2001**).

15. J. Chen, M. A. Hamon, H. Hu, Y. Chen, A. M. Rao, P. C. Eklund, and R. C. Haddon, *Science* 282, 95 (**1998**); J. Chen, A. M. Rao, S. Lyuksyutov, M. E. Itkis, M. A. Hamon, H. Hu, R. W. Cohn, P. C. Eklund, D. T. Colbert, R. E. Smalley, and R. C. Haddon, *J. Phys. Chem. B* 105, 2525 (**2001**).

16. D. E. Hill, Y. Lin, A. M. Rao, L. F. Allard, Y. Ping Sun, *Macromolecules* 35, 9466 (**2002**).

17. R. A. Forman, G. J. Piermarini, J. D. Barnett, and S. Block, *Science* 176, 284 (**1972**).

18. M. Hanfland, H. Beister, and K. Syassen, *Phys. Rev. B* 39, 12598 (**1989**).

RESEARCH ARTICLE